

Alberta Thy 06-09
SFB/CPP-09-30
TTP09-09

Completely automated computation of the heavy-fermion corrections to the three-loop matching coefficient of the vector current

P. Marquard^(a), J.H. Piclum^(b), D. Seidel^(b), M. Steinhauser^(a)

(a) Institut für Theoretische Teilchenphysik, Universität Karlsruhe (TH)

Karlsruhe Institute of Technology (KIT), 76128 Karlsruhe, Germany

(b) Department of Physics, University of Alberta, Edmonton, Alberta, Canada T6G 2G7

Abstract

We evaluate the corrections to the matching coefficient of the vector current between Quantum Chromodynamics (QCD) and Non-Relativistic QCD (NRQCD) to three-loop order containing a closed heavy-fermion loop. The result constitutes a building block both for the bottom- and top-quark system at threshold. Strong emphasis is put on our completely automated approach of the calculation including the generation of the Feynman diagrams, the identification of the topologies, the reduction to master integrals and the automated numerical computation of the latter.

PACS numbers: 12.38.Bx 12.38.-t 14.65.Ha

1 Introduction

A major goal of a future international linear collider (ILC) is the precise measurement of the top-quark production cross section close to threshold. Next to a precise extraction of the strong coupling, an unrivalled determination of the top-quark mass and its width is possible. This would open up a new chapter in the electroweak precision physics which leads to very strong checks of the Standard Model or possible extensions.

The theoretical calculation of the threshold cross section is based on an effective theory [1,2] (for a review see [3]) which is constructed from QCD by integrating out the hard scale given by the top-quark mass. The connection between the two theories is established by so-called matching coefficients which constitute the coupling constants of the effective operators within NRQCD.

A preliminary analysis to next-to-next-to-next-to leading order (NNNLO) of the top-quark threshold cross section, which is necessary in order to match the expected experimental precision [4], has been performed in Ref. [5]. However, the three-loop static potential (see Ref. [6] for the fermionic contribution) and the three-loop matching coefficient beyond the light-fermion approximation [7] are still missing. In this paper we provide a further building block needed for the completion of the NNNLO calculation: the heavy-fermion contribution to the three-loop matching coefficient. Next to important applications in the top-quark sector NRQCD is also an appropriate tool for the description of boundstate phenomena of charm and bottom quarks [3].

The matching coefficient of the vector current in the full and effective theory is defined through ($k = 1, 2, 3$)

$$j_v^k = c_v(\mu)\tilde{j}^k + \mathcal{O}\left(\frac{1}{m_Q^2}\right), \quad (1)$$

where the vector current in the full and effective theory reads

$$j_v^\mu = \bar{Q}\gamma^\mu Q, \quad \tilde{j}^i = \phi^\dagger\sigma^i\chi. \quad (2)$$

Q denotes a generic heavy quark with mass m_Q and ϕ and χ are two-component Pauli spinors for quark and anti-quark, respectively. In this paper we compute the three-loop non-singlet contribution to c_v which contains one or two closed heavy quark loops. The analog corrections involving closed light (massless) quark loops have been considered in Ref. [7].

The evaluation of the three-loop diagrams contributing to c_v is quite involved. One has to consider vertex diagrams with massive quarks on their mass shell and the external momentum $q^2 = 4m_Q^2$. This kinematical configuration in combination with an involved reduction to master integrals makes the calculation quite challenging. In this paper we discuss an automated setup which minimizes the manual interaction. Even the results for the master integrals are obtained in an automated way.

Our approach for the automated calculation is introduced in the next section. Afterwards we present the results for the matching coefficient in Section 3 and conclude in Section 4.

2 Automated multi-loop calculation

When evaluating multi-loop Feynman integrals one encounters several difficulties which have to be overcome. Among them are the generation of the Feynman diagrams, the reduction of the many integrals which appear at the initial stage of the calculation to a relatively small set of so-called master integrals and the evaluation of the latter. Very often the individual steps are automated, however, the interplay between them is not. In the following we present a setup where various program packages are combined in order to minimize the manual work.

The individual steps of our automated setup are as follows

1. All Feynman diagrams are generated with **QGRAF** [8] which requires two input files: one specifying the process and one containing the propagators and vertices occurring in the theory.
2. The output of **QGRAF** is transformed to **FORM** [9] with the help of the program **q2e** [10, 11]. **q2e** requires as input the **FORM** notation for the propagators and vertices and information about the hierarchy of the particle masses and the external momenta.
3. The output of **q2e** is further processed with **exp** which identifies the various topologies and generates for each diagram a separate file containing complete information like the projectors to be applied, the expansion to be performed and the topology file to be called.
4. In a next step the **FORM** part is initiated. After taking the traces and applying the projectors a topology-specific file is included which expresses the result in terms of a sum of scalar integrals.
5. From the sum of all diagrams a list of integrals is extracted. This list serves as input for **crusher** [12] which produces for each topology a table containing the reduction to master integrals.
6. Each topology produces a certain number of master integrals. A small **Mathematica** routine combines all master integrals, identifies identical ones and generates relations among them.
7. The tables from step 5 together with the relations among master integrals (step 6) are applied to the sum of the bare diagrams leading to a representation of the result in terms of a minimal set of master integrals multiplied with ϵ -dependent coefficients.
8. The input for **crusher** can also be used for **FIESTA** [13] which we employ in order to obtain numerical results for the master integrals.
9. At four places information about the topologies are needed: as input for **exp** (cf. step 3) and **crusher** (cf. step 5), for the topology-specific **FORM** file (cf. step 4) and for identifying identical master integrals (cf. step 6). This input is generated

automatically from a file containing the definition of the three-loop topologies for the two-point on-shell integrals entering, e.g., the $\overline{\text{MS}}$ -on-shell relation of the quark mass [14–17]. This file is available from our previous calculation [17]. Note that this is the only input which contains non-trivial problem-specific information; the remaining input files (see steps 1 and 2) are either quite generic (e.g. identical for all QCD processes) or quite simple to adapt like the specification of the process under consideration for **QGRAF**.

Let us stress that the automated setup outlined above requires little interaction from outside and thus minimizes possible errors.

Many steps of the above list have been used extensively in previous calculations, however, the automatic calculation of the master integrals is new. Such an approach is essential in those cases where many master integrals occur. In our calculation we encounter 24 master integrals for the contribution involving a closed heavy fermion loop.

Of course, a setup as described above requires several checks to be performed on the final result. On one hand they certainly include gauge parameter independence and the finiteness, on the other hand several checks on the numerical stability of our result are necessary. In our case the latter include the following:

- **FIESTA** [13], which is an efficient implementation of the sector decomposition method for the evaluation of master integrals, provides the possibility to introduce a lower cut-off in the numerical integration where numerical instabilities can occur. Actually, for the evaluation of our master integrals we have to choose a non-zero cut-off. Its variation provides an estimate of the uncertainty.
- **FIESTA** furthermore provides an uncertainty from the underlying Monte-Carlo integration performed with **Vegas** [18] which we also take into account.
- A further estimate of the uncertainty is provided by changing the basis used for the master integrals. The corresponding relations among the master integrals can be obtained in a straightforward way from the reduction tables generated by **crusher**.
- Some of the master integrals are known analytically and can thus be used to replace the corresponding numerical expressions.

3 Matching coefficient

Starting from Eq. (1) it is possible to derive the equation¹

$$Z_2 \Gamma_v = c_v \tilde{Z}_v^{-1}, \quad (3)$$

where Γ_v denotes the one-particle irreducible vertex diagrams with on-shell quarks with momenta q_1 and q_2 and $q^2 = (q_1 + q_2)^2 = 4m_Q^2$. Some sample Feynman diagrams contributing at the one-, two- and three-loop level are shown in Fig. 1. Z_2 is the wave function

¹See, e.g., Ref. [7] for a derivation based on the threshold expansion [19, 20].

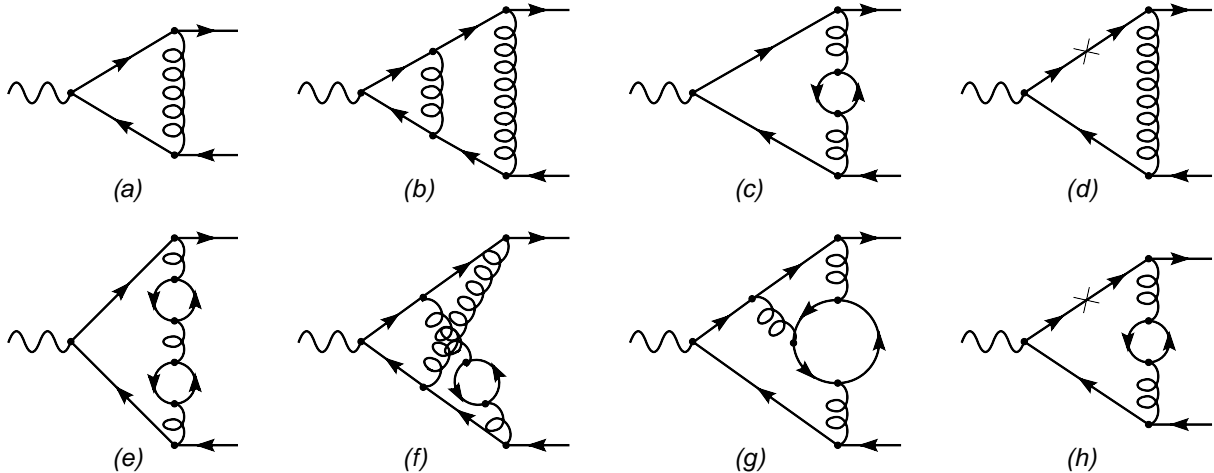


Figure 1: Feynman diagrams contributing to the matching coefficient. Solid lines denote (heavy) quarks with mass m_Q and curly lines denote gluons. In (d) and (h) mass counterterm diagrams are shown.

renormalization constant in the on-shell scheme and \tilde{Z}_v collects the infra-red divergences within the minimal subtraction scheme. The latter are cancelled against ultra-violet divergences of the effective theory rendering physical quantities finite.

The two- and three-loop corrections to Z_2 have been computed in Refs. [21] and [17,22], respectively, and \tilde{Z}_v can be obtained from Ref. [23] (see also Refs. [7,24]). The latter reads

$$\begin{aligned}
\tilde{Z}_v &= 1 + \left(\frac{\alpha_s^{(n_l)}(\mu)}{\pi} \right)^2 \left(\frac{1}{12} C_F^2 + \frac{1}{8} C_F C_A \right) \frac{\pi^2}{\epsilon} \\
&+ \left(\frac{\alpha_s^{(n_l)}(\mu)}{\pi} \right)^3 C_F T \left\{ n_l \left[\left(\frac{1}{54} C_F + \frac{1}{36} C_A \right) \frac{\pi^2}{\epsilon^2} - \left(\frac{25}{324} C_F + \frac{37}{432} C_A \right) \frac{\pi^2}{\epsilon} \right] \right. \\
&\left. + C_F n_h \frac{\pi^2}{60\epsilon} \right\} + \dots, \tag{4}
\end{aligned}$$

where $C_A = N_c$, $C_F = (N_c^2 - 1)/(2N_c)$ and $T = 1/2$ for a $SU(N_c)$ group and the ellipses stand for non-fermionic and $\mathcal{O}(\alpha_s^4)$ terms. Note that the strong coupling is defined in the effective theory with n_l active quarks where $n_l + n_h$ is the total number of quark flavours. In our case we have $n_h = 1$, however, we keep n_h in the formulae for convenience. Since there are poles starting from order α_s^2 , higher order terms in ϵ are necessary for the decoupling relation of α_s . They have been computed in Ref. [25] and can be found in explicit form in Eq. (12) of Ref. [26]. For the evaluation of Γ_v to three-loop order also one- and two-loop expressions for the strong-coupling and quark-mass counterterms are needed which have been well-known for many years (see, e.g., Ref. [17]).

The approach which has been chosen for the evaluation of the Feynman diagrams both at two-loop [27,28] and at three-loop order [7] for the light-fermion contribution is based

on a partial fractioning of the integrands. As a consequence the occurring integrals can be mapped to diagrams containing less lines. Although they are in general simpler to evaluate they contain denominators raised to higher powers which partially compensates this advantage. On the other hand, the original vertex diagrams are more complicated to evaluate, but we can use additional recurrence relations derived from the fact that the momenta of the external quarks are the same. Actually, we computed the three-loop n_l -contribution in both ways and observed no significant difference in the overall performance. Thus, in the automatic approach we refrain from performing the partial fractioning and evaluate directly the vertex diagrams.

It is convenient to cast the perturbative expansion of the matching coefficient in the form

$$c_v = 1 + \frac{\alpha_s^{(n_l)}(\mu)}{\pi} c_v^{(1)} + \left(\frac{\alpha_s^{(n_l)}(\mu)}{\pi} \right)^2 c_v^{(2)} + \left(\frac{\alpha_s^{(n_l)}(\mu)}{\pi} \right)^3 c_v^{(3)} + \mathcal{O}(\alpha_s^4), \quad (5)$$

where we further decompose $c_v^{(3)}$ according to the colour structures as

$$\begin{aligned} c_v^{(3)} &= C_F T n_l (C_F c_{FFL} + C_A c_{FAL} + T n_h c_{FHL} + T n_l c_{FLL}) \\ &\quad + C_F T n_h (C_F c_{FFH} + C_A c_{FAH} + T n_h c_{FHH}) \\ &\quad + \text{non-fermionic and singlet terms.} \end{aligned} \quad (6)$$

The one- [29] and two-loop [27, 28, 30] terms have been known for more than ten years. More recently also the three-loop corrections proportional to n_l became available [7]. The corresponding results read²

$$\begin{aligned} c_v^{(1)} &= -2C_F, \\ c_v^{(2)} &= \left(-\frac{151}{72} + \frac{89}{144}\pi^2 - \frac{5}{6}\pi^2 \ln 2 - \frac{13}{4}\zeta(3) \right) C_A C_F \\ &\quad + \left(\frac{23}{8} - \frac{79}{36}\pi^2 + \pi^2 \ln 2 - \frac{1}{2}\zeta(3) \right) C_F^2 + \left(\frac{22}{9} - \frac{2}{9}\pi^2 \right) C_F T n_h \\ &\quad + \frac{11}{18} C_F T n_l - \frac{1}{2} \left[4\beta_0 + \pi^2 \left(\frac{1}{2}C_A + \frac{1}{3}C_F \right) \right] C_F L_\mu, \\ c_{FFL} &= 46.7(1) + \left(-\frac{17}{12} + \frac{61}{36}\pi^2 - \frac{2}{3}\pi^2 \ln 2 + \frac{1}{3}\zeta(3) \right) L_\mu + \frac{1}{18}\pi^2 L_\mu^2, \\ c_{FAL} &= 39.6(1) + \left(\frac{181}{54} - \frac{67}{432}\pi^2 + \frac{5}{9}\pi^2 \ln 2 + \frac{13}{6}\zeta(3) \right) L_\mu + \left(\frac{11}{9} + \frac{1}{12}\pi^2 \right) L_\mu^2, \\ c_{FHL} &= -\frac{557}{162} + \frac{26}{81}\pi^2 + \left(-\frac{44}{27} + \frac{4}{27}\pi^2 \right) L_\mu, \\ c_{FLL} &= -\frac{163}{162} - \frac{4}{27}\pi^2 - \frac{11}{27}L_\mu - \frac{2}{9}L_\mu^2, \end{aligned} \quad (7)$$

²Note that in Ref. [7] the result has been expressed in terms of the six-flavour coupling whereas here we use $\alpha_s^{(5)}$. This explains the difference in the logarithmic part of the coefficient c_{FHL} .

	this work	Ref. [7]
$\tilde{c}_v^{(2)}$	-42.5138(2)	-42.5140
\tilde{c}_{FFL}	46.692(1)	46.7(1)
\tilde{c}_{FAL}	39.623(1)	39.6(1)
\tilde{c}_{FHL}	-0.27029(4)	-0.27025
\tilde{c}_{FLL}	-2.46833(3)	-2.46834
$\tilde{c}_v^{(3)} _{n_l}$	$n_l (120.660(3) - 0.8228n_l)$	$n_l (121. - 0.8228n_l)$

Table 1: Two-loop and light-fermion contribution to c_v . The results obtained with our numerical approach are compared to the ones of Ref. [7]. We have chosen the value 10^{-3} for the FIESTA parameter `IfCut`. n_h is set to one in the last row.

with $L_\mu = \ln(\mu^2/m_Q^2)$ and $\beta_0 = (11/3C_A - 4/3Tn_l)/4$. In this paper we consider the contributions proportional to n_h , i.e. new results for c_{FFH} , c_{FAH} and c_{FHH} are presented. We separate the logarithmic contributions and write

$$\begin{aligned}
c_{FFH} &= \tilde{c}_{FFH} - \frac{1}{20}\pi^2 L_\mu, \\
c_{FAH} &= \tilde{c}_{FAH} + \left(\frac{121}{27} - \frac{11}{27}\pi^2\right) L_\mu, \\
c_{FHH} &= \tilde{c}_{FHH},
\end{aligned} \tag{8}$$

where the L_μ term in c_{FFH} arises from Eq. (4) and the one in c_{FAH} originates from the running of α_s .

Before considering the heavy-fermion contribution let us in a first step consider the two-loop and light-fermion contribution in order to get some confidence in our approach. In Tab. 1 the results of our approach are compared to the ones of Refs. [7]. The uncertainties given in the middle column are obtained by adding the numerical uncertainties of the individual master integrals in quadrature. We observe an impressive agreement for all coefficients which is in particular true for the analytically known coefficients $\tilde{c}_v^{(2)}$, \tilde{c}_{FHL} and \tilde{c}_{FLL} . Furthermore, in the case of \tilde{c}_{FFL} and \tilde{c}_{FAL} a more precise result is obtained as compared to the approach of Ref. [7] where the Mellin-Barnes method has been used for the evaluation of the non-trivial master integrals.

The new results for the n_h contribution are shown in Tab. 2. In the column “numerical results” we show the numbers as obtained from the setup described in the previous section, i.e. there has been no manual interaction in the calculation of three-loop diagrams. On the other hand, if the master integrals which are known analytically³ are used we obtain the numbers presented in the third column of Tab. 2. One observes only marginal improvements. For this reason we use for the following discussion the numerical results for the master integrals.

³The numerical agreement between the analytically known integrals and the results from FIESTA is about four to five digits in the coefficient of the highest ϵ expansion term which enters the finite contribution of c_v .

	numerical result	semi-analytical result
$c_{\text{FFH}} _{\log}$	-0.496(2)	-0.494(1)
\tilde{c}_{FFH}	-0.841(3)	-0.840(2)
\tilde{c}_{FAH}	-0.10(2)	-0.09(2)
\tilde{c}_{FHH}	0.05126(1)	0.05124
\tilde{c}_{FHL}	-0.27029(4)	-0.27025
$\tilde{c}_v^{(3)} _{n_h}$	$-0.93(4) - 0.09010(1)n_l$	$-0.92(4) - 0.09008n_l$

Table 2: Three-loop heavy fermion contribution to c_v . For the results in the middle column we use only numerical results for the master integrals whereas in the right columns all available analytical information is employed. We have chosen the value 10^{-3} for the FIESTA parameter `IfCut`. n_h is set to one in the last row.

We have performed several checks on the correctness of our result and on the stability of the numerical calculations. In the Feynman rule for the gluon propagator we allow for a general gauge parameter and perform an expansion up to the linear term before the reduction to master integrals. The cancellation of the gauge parameter in the final result, after including counterterm contributions, serves as a welcome check for the correctness of our result. Furthermore, we have checked that both the spurious poles of order $1/\epsilon^4$ and $1/\epsilon^5$ and the $1/\epsilon^3$ and $1/\epsilon^2$ poles in our final expression cancel with an accuracy of about 10^{-4} .

As a further test on the numerical stability of the evaluation of the master integrals we vary the parameter `IfCut`. In Fig. 2 the results for \tilde{c}_{FFH} and \tilde{c}_{FAH} are shown for several values between `IfCut`= $5 \cdot 10^{-5}$ and `IfCut`= 0.1 where for the guidance of the eye the data points are connected by straight lines. One observes a broad plateau with only very minor variations. Larger deviations are obtained at the end points where either the value for `IfCut` becomes too big or numerical instabilities occur at the lower end of the integration region. Note that the CPU time for the evaluation of the master integrals with FIESTA varies from one to several days, depending on the setting for `Vegas`.

As a further check on the numerical evaluation of the master integrals we have used a different momentum assignment in the input for FIESTA. As a consequence different expressions are generated in intermediate steps leading to different numerical integrations. The final results are in agreement with the ones in Tab. 2 within a one sigma level.

A strong check on the numerical results for the master integrals is provided by a change of the master integral basis. We replace the complicated integrals by other integrals which we again evaluate with FIESTA. The relations between the old and new integrals can be extracted from the tables produced by `crusher`. By changing the basis two times (cf. Eqs. (13) and (14)) we obtain the results given in Tab. 3. We find good agreement with the results of Tab. 2 for all coefficients. Let us mention that in the standard basis spurious poles of at most fourth order arise whereas both for basis 2 and 3 $1/\epsilon^5$ poles are present in our result. Let us furthermore stress that the integrals for the new bases are significantly

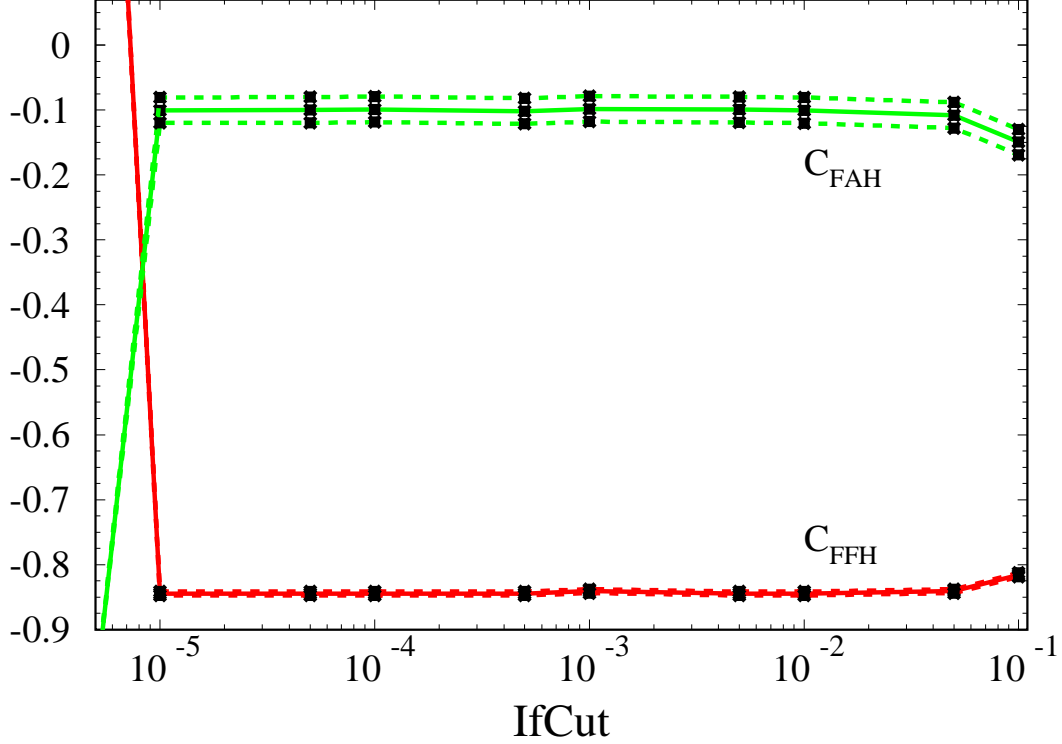


Figure 2: Coefficients \tilde{c}_{FFH} and \tilde{c}_{FAH} as a function of `IfCut` (choosing `VarExpansionDegree=1`). The band corresponds to the numerical uncertainty as provided by FIESTA.

more complicated due to the higher powers of the propagators. This explains the slightly worse numerical precision of the results in Tab. 3.

Our final result for $c_v^{(3)}$ reads

$$\begin{aligned}
 \tilde{c}_{FFH} &= -0.841(6), \\
 \tilde{c}_{FAH} &= -0.10(4), \\
 \tilde{c}_{FHH} &= -\frac{427}{162} + \frac{158}{2835}\pi^2 + \frac{16}{9}\zeta(3) \approx 0.05124,
 \end{aligned}
 \tag{9}$$

where the values for \tilde{c}_{FFH} and \tilde{c}_{FAH} are taken from Tab. 2. The uncertainties are conservatively estimated by doubling the error from the numerical integration. In this way we account for effects connected to the FIESTA parameter `IfCut`, to different momenta assignments in the input of FIESTA, and the change of the master integral basis. The need for doubling the error can also be seen by comparing the two values for \tilde{c}_{FHH} in Tab. 2.

Inserting the numerical values for the colour factors we obtain for $\mu = m_Q$

$$c_v^{(3)} \approx -0.823 n_l^2 + 120.66(1) n_l - 0.93(8) + \text{non-fermionic and singlet terms}. \tag{10}$$

	basis 2 Eq. (13)	basis 3 Eq. (14)
$c_{\text{FFH}} _{\log}$	-0.50(1)	-0.496(8)
\tilde{c}_{FFH}	-0.85(6)	-0.86(2)
\tilde{c}_{FAH}	-0.15(9)	-0.13(4)
\tilde{c}_{FHH}	0.0513(1)	0.0513(1)
\tilde{c}_{FHL}	-0.27028(3)	-0.2703(2)
$\tilde{c}_v^{(3)} _{n_h}$	-1.04(23) - 0.09009(1) n_l	-1.00(11) - 0.09009(5) n_l

Table 3: Three-loop heavy fermion contribution to c_v . For the master integrals which are only available in numerical form the sets given in Eqs. (13) and (14) have been used. We have chosen the value 10^{-3} for the FIESTA parameter `IfCut`. n_h is set to one in the last row.

It turns out the numerical coefficient of the heavy-fermion contribution is comparable with the n_l^2 part, however, significantly smaller than the coefficient of the linear n_l term.

4 Conclusions and outlook

In this paper we discussed a completely automated approach for the calculation of three-loop vertex corrections contributing to the matching coefficients of the vector current, c_v . In particular we consider the Feynman diagrams containing a closed heavy fermion loop which lead to significantly more complicated integrals than the light-fermion contributions considered more than two years ago [7]. We have shown that numerically stable results are obtained even for the case where all ϵ coefficients of all 24 master integrals are evaluated numerically. Furthermore, we were able to improve the precision of the light-fermion contribution. The method developed in this work will be crucial for the three-loop non-fermionic and singlet contributions to c_v which are still unknown.

Our automated approach depends crucially on the fact that FIESTA is able to evaluate the master integrals to a sufficiently high accuracy. To make sure of this, we have checked that FIESTA reproduces all analytically known results within the given errors. In addition, we have performed the calculation of the matching coefficient in three different master integral bases and find consistent results. This makes us confident that our result is correct within the given error bar.

Acknowledgements

We would like to thank A. Czarnecki and A.A. Penin for useful comments and discussions and A.V. Smirnov for continuous support on FIESTA. This work was supported by the DFG through SFB/TR 9. The work of JHP and DS is supported by Science and Engineering Research Canada and the Alberta Ingenuity Fund. The Feynman diagrams were drawn with the help of Axodraw [31] and JaxoDraw [32].

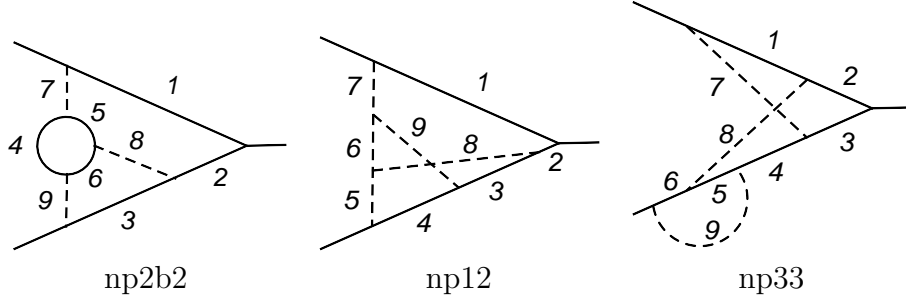


Figure 3: Generic vertex diagrams where the solid and dashed lines correspond to massive and massless propagators, respectively. The external momenta are set to $4m_Q^2$ (out-going on the right-hand side) and m_Q^2 (in-coming on the left-hand side), respectively. For V_{np12} and V_{np33} closed fermion contributions are generated by contracting massless lines.

Appendix: master integrals

In this appendix we list the 24 master integrals which we encounter in the calculation for the n_h contribution to c_v . We refrain from providing explicit results since they can either be found in analytical form in the cited literature or can be obtained in numerical form using FIESTA [13].

There are twelve master integrals which are known in analytical form to a sufficiently high power in the ϵ expansion. They are given by

$$\begin{aligned}
& V_{np2b2}(0, 1, 0, 1, 1, 0, 0, 1, 1), V_{np2b2}(0, 1, 0, 1, 1, 1, 0, 1, 1), V_{np2b2}(0, 1, 1, 0, 1, 1, 0, 0, 0), \\
& V_{np2b2}(0, 1, 1, 0, 1, 1, 1, 0, 1), V_{np2b2}(0, 1, 1, 1, 1, 0, 0, 0, 0), V_{np2b2}(0, 1, 1, 1, 1, 0, 0, 1, 1), \\
& V_{np2b2}(0, 1, 1, 1, 1, 1, 0, 0, 0), V_{np12}(0, 1, 1, 1, 0, 0, 0, 0, 0), V_{np12}(0, 1, 1, 0, 1, 0, 0, 0, 1), \\
& V_{np12}(0, 1, 1, 0, 1, 1, 0, 0, 0), V_{np12}(0, 1, 1, 1, 0, 1, 0, 0, 0), V_{np12}(1, 0, 1, 1, 0, 0, 0, 1, 0),
\end{aligned} \tag{11}$$

where V_{np2b2} and V_{np12} are given in graphical form in Fig. 3. The numbers next to the lines mark the corresponding indices. The results for these integrals can be found in Refs. [22, 33] (see also [7]).

The poles of the integral $V_{np2b2}(1, 0, 1, 0, 1, 1, 0, 0, 0)$ can be found in Ref. [34]; the finite part is computed with FIESTA.

The following eleven integrals are only known numerically with the help of FIESTA

$$\begin{aligned}
& V_{np2b2}(1, 0, 1, 0, 1, 1, 1, 0, 1), V_{np2b2}(1, 0, 1, 0, 1, 2, 0, 0, 0), V_{np2b2}(1, 0, 1, 1, 0, 1, 0, 1, 0), \\
& V_{np2b2}(1, 0, 1, 1, 0, 1, 0, 2, 0), V_{np2b2}(1, 0, 1, 1, 0, 1, 1, 1, 0), V_{np2b2}(1, 0, 1, 1, 1, 1, 0, 0, 0), \\
& V_{np2b2}(1, 0, 1, 1, 1, 1, 0, 1, 0), V_{np2b2}(1, 0, 1, 1, 1, 1, 0, 2, 0), V_{np33}(0, 1, 1, 1, 1, 1, 1, 0, 0), \\
& V_{np33}(1, 1, 0, 1, 1, 1, 1, 0, 0), V_{np33}(1, 1, 1, 0, 1, 1, 0, 0, 1).
\end{aligned} \tag{12}$$

The change of the master integral basis discussed in Section 3 affects only the integrals in Eq. (12), $V_{np2b2}(1, 0, 1, 0, 1, 1, 0, 0, 0)$ and the last five integrals in Eq. (11) which are

replaced by either (“basis 2”)

$$\begin{aligned}
& V_{np12}(0, 2, 1, 0, 1, 0, 0, 0, 1), V_{np12}(0, 2, 1, 0, 1, 1, 0, 0, 0), V_{np12}(0, 2, 1, 1, 0, 1, 0, 0, 0), \\
& V_{np12}(1, 0, 2, 1, 0, 0, 0, 1, 0), V_{np12}(2, 0, 1, 1, 0, 0, 0, 1, 0), V_{np2b2}(1, 0, 1, 0, 1, 1, 1, 0, 2), \\
& V_{np2b2}(1, 0, 1, 0, 1, 2, 1, 0, 1), V_{np2b2}(1, 0, 1, 0, 1, 3, 0, 0, 0), V_{np2b2}(1, 0, 1, 1, 0, 1, 0, 3, 0), \\
& V_{np2b2}(1, 0, 1, 1, 0, 1, 1, 2, 0), V_{np2b2}(1, 0, 1, 1, 0, 1, 2, 1, 0), V_{np2b2}(1, 0, 1, 1, 1, 1, 0, 3, 0), \\
& V_{np2b2}(1, 0, 1, 1, 1, 2, 0, 0, 0), V_{np2b2}(1, 0, 1, 1, 1, 2, 0, 1, 0), V_{np2b2}(1, 0, 1, 1, 1, 2, 0, 2, 0), \\
& V_{np33}(0, 2, 1, 1, 1, 1, 1, 0, 0), V_{np33}(2, 1, 0, 1, 1, 1, 1, 0, 0), V_{np33}(2, 1, 1, 0, 1, 1, 0, 0, 1),
\end{aligned} \tag{13}$$

or (“basis 3”)

$$\begin{aligned}
& V_{np12}(0, 1, 1, 0, 1, 0, 0, 0, 2), V_{np12}(0, 1, 1, 0, 1, 2, 0, 0, 0), V_{np12}(0, 1, 1, 1, 0, 2, 0, 0, 0), \\
& V_{np12}(1, 0, 1, 1, 0, 0, 0, 2, 0), V_{np12}(1, 0, 2, 1, 0, 0, 0, 1, 0), V_{np2b2}(1, 0, 1, 0, 1, 1, 2, 0, 1), \\
& V_{np2b2}(1, 0, 1, 0, 2, 1, 0, 0, 0), V_{np2b2}(1, 0, 1, 0, 2, 1, 1, 0, 1), V_{np2b2}(1, 0, 1, 1, 0, 2, 0, 1, 0), \\
& V_{np2b2}(1, 0, 1, 1, 0, 2, 0, 2, 0), V_{np2b2}(1, 0, 1, 1, 0, 2, 1, 1, 0), V_{np2b2}(1, 0, 1, 1, 1, 2, 0, 1, 0), \\
& V_{np2b2}(1, 0, 1, 1, 2, 1, 0, 0, 0), V_{np2b2}(1, 0, 1, 1, 2, 1, 0, 1, 0), V_{np2b2}(1, 0, 1, 1, 2, 1, 0, 2, 0), \\
& V_{np33}(0, 1, 1, 1, 1, 1, 2, 0, 0), V_{np33}(1, 1, 0, 1, 1, 1, 2, 0, 0), V_{np33}(1, 1, 1, 0, 1, 1, 0, 0, 2).
\end{aligned} \tag{14}$$

Note that both basis 2 and 3 contain one more master integral than our standard basis. This is because the latter in principle also contains the integral $V_{np2b2}(1, 0, 1, 1, 1, 2, 0, 1, 0)$, however, for our application the corresponding coefficient is zero.

References

- [1] W. E. Caswell and G. P. Lepage, Phys. Lett. B **167** (1986) 437.
- [2] G. T. Bodwin, E. Braaten and G. P. Lepage, Phys. Rev. D **51** (1995) 1125 [Erratum-ibid. D **55** (1997) 5853] [arXiv:hep-ph/9407339].
- [3] N. Brambilla *et al.*, arXiv:hep-ph/0412158.
- [4] M. Martinez and R. Miquel, Eur. Phys. J. C **27** (2003) 49 [arXiv:hep-ph/0207315].
- [5] M. Beneke, Y. Kiyo and K. Schuller, PoS **RADCOR2007** (2007) 051 [arXiv:0801.3464 [hep-ph]].
- [6] A. V. Smirnov, V. A. Smirnov and M. Steinhauser, Phys. Lett. B **668** (2008) 293 [arXiv:0809.1927 [hep-ph]].
- [7] P. Marquard, J. H. Piclum, D. Seidel and M. Steinhauser, Nucl. Phys. B **758** (2006) 144 [arXiv:hep-ph/0607168].

- [8] P. Nogueira, *J. Comput. Phys.* **105** (1993) 279.
- [9] J. A. M. Vermaseren, arXiv:math-ph/0010025.
- [10] R. Harlander, T. Seidensticker and M. Steinhauser, *Phys. Lett. B* **426** (1998) 125 [hep-ph/9712228].
- [11] T. Seidensticker, hep-ph/9905298.
- [12] P. Marquard and D. Seidel, unpublished.
- [13] A. V. Smirnov and M. N. Tentyukov, arXiv:0807.4129 [hep-ph].
- [14] K. G. Chetyrkin and M. Steinhauser, *Nucl. Phys. B* **573** (2000) 617 [arXiv:hep-ph/9911434].
- [15] K. G. Chetyrkin and M. Steinhauser, *Phys. Rev. Lett.* **83** (1999) 4001 [arXiv:hep-ph/9907509].
- [16] K. Melnikov and T. v. Ritbergen, *Phys. Lett. B* **482** (2000) 99 [arXiv:hep-ph/9912391].
- [17] P. Marquard, L. Mihaila, J. H. Piclum and M. Steinhauser, *Nucl. Phys. B* **773** (2007) 1 [arXiv:hep-ph/0702185].
- [18] G. P. Lepage, *J. Comput. Phys.* **27** (1978) 192.
- [19] M. Beneke and V. A. Smirnov, *Nucl. Phys. B* **522** (1998) 321 [arXiv:hep-ph/9711391].
- [20] V. A. Smirnov, “Applied asymptotic expansions in momenta and masses,” Springer (2002).
- [21] D. J. Broadhurst, N. Gray and K. Schilcher, *Z. Phys. C* **52** (1991) 111.
- [22] K. Melnikov and T. van Ritbergen, *Nucl. Phys. B* **591** (2000) 515 [arXiv:hep-ph/0005131].
- [23] B. A. Kniehl, A. A. Penin, M. Steinhauser and V. A. Smirnov, *Phys. Rev. Lett.* **90** (2003) 212001 [Erratum-ibid. **91** (2003) 139903(E)] [arXiv:hep-ph/0210161].
- [24] M. Beneke, Y. Kiyo and A. A. Penin, *Phys. Lett. B* **653** (2007) 53 [arXiv:0706.2733 [hep-ph]].
- [25] K. G. Chetyrkin, B. A. Kniehl and M. Steinhauser, *Nucl. Phys. B* **510** (1998) 61 [arXiv:hep-ph/9708255].
- [26] A. G. Grozin, P. Marquard, J. H. Piclum and M. Steinhauser, *Nucl. Phys. B* **789** (2008) 277 [arXiv:0707.1388 [hep-ph]].

- [27] A. Czarnecki and K. Melnikov, Phys. Rev. Lett. **80** (1998) 2531 [arXiv:hep-ph/9712222].
- [28] M. Beneke, A. Signer and V. A. Smirnov, Phys. Rev. Lett. **80** (1998) 2535 [arXiv:hep-ph/9712302].
- [29] G. Källén and A. Sarby, K. Dan. Vidensk. Selsk. Mat.-Fis. Medd. 29, N17 (1955) 1.
- [30] B. A. Kniehl, A. Onishchenko, J. H. Piclum and M. Steinhauser, Phys. Lett. B **638** (2006) 209 [arXiv:hep-ph/0604072].
- [31] J. A. M. Vermaseren, Comput. Phys. Commun. **83** (1994) 45.
- [32] D. Binosi and L. Theussl, Comput. Phys. Commun. **161** (2004) 76 [arXiv:hep-ph/0309015].
- [33] S. Laporta and E. Remiddi, Phys. Lett. B **379** (1996) 283 [arXiv:hep-ph/9602417].
- [34] S. Groote, J. G. Korner and A. A. Pivovarov, Eur. Phys. J. C **36** (2004) 471 [arXiv:hep-ph/0403122].